Adaptive State Constrained Control of a Flexible Riser System With Transient Performance

Xin-Yu Zhang, Xiangpeng Xie, *Senior Member, IEEE*, Yan-Jun Liu, *Senior Member, IEEE*, Li Tang, *Member, IEEE*, and Zhou Gu, *Senior Member, IEEE*

***Abstract*—A novel adaptive constraint control approach is proposed for flexible riser systems characterized by uncertain parameters and external disturbances, aimed at achieving the desired transient performance. By combining Hamilton's principle with partial differential equations (PDEs), the physical model is transformed into a dynamic model. Considering the boundary position constraint, a boundary controller is built using the tangent barrier Lyapunov function (BLF) to mitigate vibrations. In order to ensure the convergence of the boundary position error at a predetermined rate, the control approach incorporates a performance function to attain the necessary transient performance. An auxiliary term is defined to counteract the impact of coupling terms that remain during the decoupling process of PDEs. Finally, the above scheme is further validated through MATLAB simulations.**

***Index Terms*—Adaptive control, boundary position constraint, partial differential equations (PDEs), tangent barrier Lyapunov function (BLF), transient performance.**

I. Introduction

In real-life physical systems, uncertain disturbances generated by external environments inevitably, lead to significant degradation of system performance. To address this issue, various control methods are proposed, including neural network control [1], [2], [3], [4], robust control [5], [6], fuzzy logic control [7], [8], and adaptive control [9], [10], [11], [12]. For instance, in [2], a robust optimal control method is designed for uncertain nonlinear systems by integrating neural networks and adaptive critic techniques. An embedded adaptive robust controller is proposed in [3] to tackle trajectory tracking and stabilization issues for omnidirectional mobile platforms. In [5], a barrier sliding mode control scheme is explored to achieve asymptotic convergence of states, addressing stability and full-state constraints. Adaptive control, distinct from other control methods, ensures system performance under uncertainty by providing appropriate gains. Tong et al. [9] developed an adaptive fuzzy output feedback control strategy for a MIMO nonlinear system with unmeasurable states by merging adaptive back-stepping and DSC technology. Under any switching condition, a simple adaptive controller is proposed in [10] to achieve effective tracking performance within a finite time. In [11], an adaptive back-stepping consensus control for recursive neural networks is explored for formation control. Tong et al. [12] proposed a fuzzy observer utilizing an adaptive control scheme to estimate unmeasurable states. For nonlinear multiagent systems, a distributed adaptive control scheme is established in [13] to mitigate the effects of time delays and noise. Hence, adaptive control stands out as an effective tool for managing uncertain systems.

When dealing with uncertainty through adaptive control, it is crucial to consider the system's constraints. Ignoring these constraints can lead to reduced efficiency and even pose safety risks. The barrier Lyapunov function (BLF) is commonly used to address constraint issues, including logarithmic BLF [14], [15], tangent BLF [16], [17], [18], and integral BLF [19]. In [20], a time-varying BLF is utilized to ensure that the constrained subsystem states remain within the set bounds. Logarithmic BLFs are employed in [14] and [15] to handle state constraints. For strictly feedback nonlinear systems, the control methods based on symmetric and asymmetric tangent BLF in [21] ensure that the output constraints are not exceeded. Compared to the conservative nature of logarithmic BLF, tangent BLF offers less conservatism, thus providing better control performance. Despite being widely used in ordinary differential equations (ODEs), the application of tangent BLF in partial differential equations (PDEs) remains relatively limited due to their spatio-temporal coupling nature.

ODEs are often inadequate for capturing the dynamic processes of industrial systems, whereas PDEs can more accurately describe real systems. Boundary control [22], [23], [24] or domain control [25], [26] is commonly used for modeling practical systems. In [27], specific boundary control methods are designed for flexible riser systems to manage both measurable and unmeasurable states, ensuring that the riser's elastic deflection remains within bounds. For the n-link robot system in [28], a single-parameter adaptive boundary control approach is adopted to address system parameter uncertainties

Received 6 November 2023; revised 7 April 2024, 28 August 2024, and 24 November 2024; accepted 26 February 2025. This work was supported in part by the National Natural Science Foundation of China under Grant 62373196. This article was recommended by Associate Editor C.-C. Tsai. *(Corresponding author: Xiangpeng Xie.)*

Xin-Yu Zhang is with the College of Automation and the College of Artificial Intelligence, Nanjing University of Posts and Telecommunications, Nanjing 210023, China (e-mail: zhangxinyu1220@hotmail.com).

Xiangpeng Xie is with the School of Internet of Things, Nanjing University of Posts and Telecommunications, Nanjing 210023, China (e-mail: xiexiangpeng1953@163.com).

Yan-Jun Liu and Li Tang are with the College of Science, Liaoning University of Technology, Jinzhou 121001, China (e-mail: liuyanjun@live.com; tangli413@hotmail.com).

Zhou Gu is with the College of Mechanical and Electronic Engineering, Nanjing Forestry University, Nanjing 210037, China (e-mail: gzh1808@163.com).

Digital Object Identifier 10.1109/TSMC.2025.3547054

and saturation constraints, thus avoiding the need to determine uncertain parameter values. Vibration problems, which often affect stability and operational accuracy in practical systems, are managed differently depending on the control method. Different from domain control, boundary control is widely applied to achieve rapid attenuation of vibrations. The complex external environment surrounding riser systems results in intricate stress distributions and significant intervariable coupling, thus greatly increasing the modeling complexity of these systems. Therefore, this article considers boundary control for flexible risers modeled using PDEs.

In industrial applications, it is essential to ensure the transient performance regulation of maritime risers. This involves rapid vessel positioning and the mitigation of system vibrations. Due to parameter uncertainties and external disturbances, achieving rapid convergence of position errors to the origin remains a tough challenge for real systems described with PDEs. A number of study findings concentrate on flexible structures. In [29], a partially actuated gantry crane is engineered to guarantee that errors converge to a minimal range close to zero at a predetermined pace by altering the variables, taking into account unmodeled dynamics and external disturbances. An iterative learning control law is proposed for monitoring desired trajectories in flexible robotic arm systems with output limits, as discussed in [30]. Chen et al. [31] utilized an adaptive approach to mitigate the cumulative impacts of disturbances and input saturation on unidentified near-space spacecraft. This article further investigates adaptive boundary control for flexible riser systems to guarantee transient performance under unknown external disturbances and state constraints.

The main contribution is as follows.

1) A novel adaptive boundary control method is proposed, which ensures fast convergence of the boundary position errors and suppresses boundary vibrations without violating constraint conditions. This method not only solves the boundary constraint problem of flexible riser systems but also ensures transient performance under parameter uncertainties and external disturbances.
2) The tangent BLF is utilized to constrain the system boundary position. To the best of our knowledge, control methods for flexible riser systems based on tangent BLF are relatively rare, primarily due to the inherent complex spatio-temporal coupling in PDEs.
3) Compared with the control strategy proposed in [22], which solely guarantees that system states meet the constraint conditions and that closed-loop system signals are bounded, we introduce a performance function that facilitates a more rapid convergence of the boundary position error to steady-state.

The remainder of this article is summarized in the following. Section II describes the model of the riser system modeled with PDE and the subsequent theory required. Section III demonstrates the controller design and system stability analysis. Section IV presents the simulation examples. Finally, Section V summarizes this article.

Notation 1: The symbol definitions are as follows (taking first-order derivatives as an example): $w'(\cdot)$ represents $\partial w(\cdot)/\partial x$, $\dot{w}(\cdot)$ represents $\partial w(\cdot)/\partial t$.

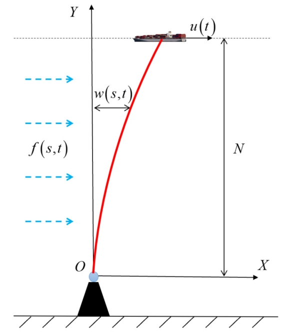

Fig. 1. Structure of a flexible riser.

II. PDE Modeling and Problem Formulation

The flexible riser system is modeled in this section, which is based on the typical characteristics of Euler-Bernoulli beams and Hamilton's principle. In the process of dynamic analysis, the ship and riser in Fig. 1 are analyzed together with the force.

The kinetic energy E_k is

$$E_k = \frac{1}{2}M\dot{w}(N,t)^2 + \frac{1}{2}\rho\int_0^N \dot{w}(s,t)^2 ds \tag{1}$$

where t and s mean independent time and space variables, respectively. The meanings of other symbols are the displacement $w(s,t)$ at s at t, ship mass M, riser length N and mass of riser per unit length ρ.

The potential energy E_p is

$$E_p = \frac{1}{2}EI\int_0^N w''(s,t)^2 ds + \frac{1}{2}T\int_0^N w'(s,t)^2 ds \tag{2}$$

where, the tension force T and flexural stiffness EI.

W is the virtual work done by the disturbing riser as

$$\begin{aligned}\delta W = &\int_0^N (f(s,t) - c\dot{w}(s,t))\delta w(s,t)ds\\ &+ (u(t) + d(t) - d_s\dot{w}(N,t))\delta w(N,t)\end{aligned} \tag{3}$$

where $f(s,t)$ is the current distribution perturbation, $u(t)$ is the control input. d_s and c are the ship and riser damping coefficients, respectively.

The Hamiltonian's principle $\int_{t_1}^{t_2}(\delta E_k - \delta E_p + \delta W)dt = 0$, which has the advantage of automatically generating boundary conditions, is employed to derive the dynamic model. Applying the variational operator and integrating (1)–(3) in fractions, respectively. We get the kinetic energy E_k as

$$\begin{aligned}\int_{t_1}^{t_2}\delta E_k dt = &\int_{t_1}^{t_2}\delta\left(\frac{1}{2}M\dot{w}(N,t)^2\right)dt\\ &+ \int_{t_1}^{t_2}\delta\left(\frac{1}{2}\rho\int_0^N \dot{w}(s,t)^2 ds\right)dt\end{aligned} \tag{4}$$

where t_1 and t_2 are different time instants, δ is defined as the variational operator.

For the first term of the E_k

$$\begin{aligned}E_{k1} &= \int_{t_1}^{t_2}\left(\delta\left(\frac{1}{2}M\dot{w}(N,t)\right)\dot{w}(N,t)\right)dt\\&\quad+\int_{t_1}^{t_2}\left(\frac{1}{2}M\dot{w}(N,t)\delta(\dot{w}(N,t))\right)dt\\&=\int_{t_1}^{t_2}(M\dot{w}(N,t)\delta(\dot{w}(N,t)))dt\\&=-\int_{t_1}^{t_2}(M\ddot{w}(N,t)\delta(w(N,t)))dt.\end{aligned}\tag{5}$$

For the second term of the E_k

$$\begin{aligned}E_{k2} &= \int_{t_1}^{t_2}\left(\int_0^N\delta\left(\frac{1}{2}\rho\dot{w}(s,t)\right)\dot{w}(s,t)ds\right)dt\\&\quad+\int_{t_1}^{t_2}\left(\int_0^N\frac{1}{2}\rho\dot{w}(s,t)\delta(\dot{w}(s,t))ds\right)dt\\&=-\int_{t_1}^{t_2}\left(\int_0^N\rho\ddot{w}(s,t)\delta(w(s,t))ds\right)dt.\end{aligned}\tag{6}$$

So, combining (5) and (6), we obtain

$$\begin{aligned}\int_{t_1}^{t_2}\delta E_k dt &= -\int_{t_1}^{t_2}(M\ddot{w}(N,t)\delta(w(N,t)))dt\\&\quad-\int_{t_1}^{t_2}\left(\int_0^N\rho\ddot{w}(s,t)\delta(w(s,t))ds\right)dt.\end{aligned}\tag{7}$$

The potential energy E_p caused by bending is

$$\begin{aligned}\int_{t_1}^{t_2}\delta E_p dt &= \int_{t_1}^{t_2}\delta\left(\frac{1}{2}EI\int_0^N w''(s,t)^2 ds\right)dt\\&\quad+\int_{t_1}^{t_2}\delta\left(\frac{1}{2}T\int_0^N w'(s,t)^2 ds\right)dt.\end{aligned}\tag{8}$$

For the first term of the E_p

$$\begin{aligned}E_{p1} &= \int_{t_1}^{t_2}\left(EI\int_0^N w''(s,t)\delta w''(s,t)ds\right)dt\\&=\int_{t_1}^{t_2}\big(EIw''(N,t)\delta w'(N,t)\big)dt\\&\quad-\int_{t_1}^{t_2}\big(EIw'''(N,t)\delta w(N,t)\big)dt\\&\quad+\int_{t_1}^{t_2}\left(EI\int_0^N w''''(s,t)\delta w(s,t)ds\right)dt.\end{aligned}\tag{9}$$

For the second term of the E_p

$$\begin{aligned}E_{p2} &= \int_{t_1}^{t_2}\left(Tw'(s,t)\delta w(s,t)\big|_0^N\right)dt\\&\quad-\int_{t_1}^{t_2}\left(T\int_0^N w''(s,t)\delta w(s,t)ds\right)dt\\&=\int_{t_1}^{t_2}\big(Tw'(N,t)\delta w(N,t)\big)dt\\&\quad-\int_{t_1}^{t_2}\left(T\int_0^N w''(s,t)\delta w(s,t)ds\right)dt.\end{aligned}\tag{10}$$

Combining (9) and (10), we obtain

$$\begin{aligned}\int_{t_1}^{t_2}\delta E_p dt &= \int_{t_1}^{t_2}\big(EIw''(N,t)\delta w'(N,t)\big)dt\\&\quad-\int_{t_1}^{t_2}\big(EIw'''(N,t)\delta w(N,t)\big)dt\\&\quad+\int_{t_1}^{t_2}\left(EI\int_0^N w''''(s,t)\delta w(s,t)ds\right)dt\\&\quad-\int_{t_1}^{t_2}\left(T\int_0^N w''(s,t)\delta w(s,t)ds\right)dt\\&\quad+\int_{t_1}^{t_2}\big(Tw'(N,t)\delta w(N,t)\big)dt.\end{aligned}\tag{11}$$

The total imaginary work W of the riser consists of the imaginary work done by the perturbation and the work done by the control inputs that suppress the transverse vibration at the boundary position, as

$$\begin{aligned}&\int_{t_1}^{t_2}\delta W dt\\&\quad=\int_{t_1}^{t_2}\int_0^N(f(s,t)-c\dot{w}(s,t))\delta w(s,t)dsdt\\&\qquad+\int_{t_1}^{t_2}(u(t)+d(t)-d_s\dot{w}(N,t))\delta w(N,t)dt.\end{aligned}\tag{12}$$

According to the Hamilton principle $\int_{t_1}^{t_2}(\delta E_k-\delta E_p+\delta W)dt=0$, (7), (11) and (12), it is obtained that

$$\begin{aligned}&\int_{t_1}^{t_2}\big(\delta E_k-\delta E_p+\delta W\big)dt\\&\quad=-\int_{t_1}^{t_2}(M\ddot{w}(N,t)\delta(w(N,t)))dt\\&\qquad-\int_{t_1}^{t_2}\left(\int_0^N\rho\ddot{w}(s,t)\delta(w(s,t))ds\right)dt\\&\qquad+\int_{t_1}^{t_2}\big(EIw''(N,t)\delta w'(N,t)\big)dt\\&\qquad+\int_{t_1}^{t_2}\big(EIw'''(N,t)\delta w(N,t)\big)dt\\&\qquad-\int_{t_1}^{t_2}\left(EI\int_0^N w''''(s,t)\delta w(s,t)ds\right)dt\\&\qquad-\int_{t_1}^{t_2}\big(Tw'(N,t)\delta w(N,t)\big)dt\\&\qquad+\int_{t_1}^{t_2}\left(T\int_0^N w''(s,t)\delta w(s,t)ds\right)dt\\&\qquad+\int_{t_1}^{t_2}\int_0^N(f(s,t)-c\dot{w}(s,t))\delta w(s,t)dsdt\\&\qquad+\int_{t_1}^{t_2}(u(t)+d(t)-d_s\dot{w}(N,t))\delta w(N,t)dt\\&\quad=0\end{aligned}\tag{13}$$

we obtain

$$\begin{aligned}&\rho\ddot{w}(s,t)-Tw''(s,t)+EIw''''(s,t)-f(s,t)\\&\quad+c\dot{w}(s,t)=0\end{aligned}\tag{14}$$

$$w'(0,t)=w''(N,t)=w(0,t)=0\tag{15}$$

$$\begin{aligned}&M\ddot{w}(N,t)-EIw'''(N,t)+Tw'(N,t)+d_s\dot{w}(N,t)\\&\quad=u(t)+d(t).\end{aligned}\tag{16}$$

The boundary positions $w(N, t)$ are all limited to the region $-k_c < w(N, t) < k_c$, where $k_c > 0$ is a constant. Furthermore, the initial condition is satisfied by $-k_c < w(N, 0) < k_c$.

Assumption 1: Suppose there are two positive constants $\bar{F}$ and D, satisfying $|f(s, t)| \leq \bar{F}$, $|d(t)| \leq D$ $\forall(s, t) \in [0, N] \times [0, +\infty)$.

Since D is bounded and unknown, we need to estimate D. Designate the estimation error of the external disturbance as

$$\tilde{D} = \hat{D} - D \tag{17}$$

where $\hat{D}$ is the adaptive law.

Define the boundary position error $e(t) = w(N, t) - w_d$, where w_d represents the desired constant boundary vibration.

Assumption 2: There is a constant $k_b > 0$ that satisfies

$$|e(0)| = |w(N, 0) - w_d| < k_b. \tag{18}$$

To guarantee that the boundary position error converges to the designated performance, we propose the following performance function, drawing inspiration from [32]

$$\beta(t) = (\beta_0 - \beta_\infty)e^{-lt} + \beta_\infty \tag{19}$$

where $\beta(t)$ is the performance function. β_0, β_∞, and l are adjustable bounded positive parameters. $\beta_0 \geq k_b$. That is, the system achieves the desired performance when the boundary position error $e(t) < \beta(t)$.

For the convenience of controller design, the error transformation function is introduced as

$$e(t) = \beta(t)\frac{e^{\phi(t)} - e^{-\phi(t)}}{e^{\phi(t)} + e^{-\phi(t)}} \tag{20}$$

where $\phi(t)$ is the transformation error. After the inverse transformation of (20), we get

$$\phi(t) = \frac{1}{2}\ln\left(\frac{1 + e(t)/\beta(t)}{1 - e(t)/\beta(t)}\right). \tag{21}$$

Control Objective: A boundary control strategy with transient performance is developed for the flexible riser (14) and boundary conditions (15) and (16) to ensure that: 1) the designed control scheme suppresses the vibration at the system boundary and the constraints are not violated; 2) the position error can converge quickly; 3) the boundary position $w(N, t)$ can be bounded.

Lemma 1 [33]: There is $G(s, t) \in \Re$ $\forall(s, t) \in [0, N] \times [0, \infty)$ satisfying $G(0, t) = 0$. So, we believe

$$G^2 \leq N\int_0^N G'^2 ds \tag{22}$$

$$G'^2 \leq N\int_0^N G_2'' ds. \tag{23}$$

Lemma 2 [34]: The inequality holds for $\xi > 0$ and $D \in \Re$

$$0 \leq |D| - D\tanh\left(\frac{D}{\xi}\right) \leq 0.2785\xi. \tag{24}$$

Lemma 3 [35]: Let $P_1(s, t), P_2(s, t) \in \Re$ with $(s, t) \in [0, N] \times [0, \infty)$, they must adhere to the following condition:

$$P_1P_2 \leq |P_1P_2| \leq \frac{1}{\varepsilon}{P_1}^2 + \varepsilon{P_2}^2.$$

III. Main Results

In this section, we present the detailed process of controller design. Furthermore, the stability analysis is based on the stability methods of PDEs.

Choose the Lyapunov function candidate as

$$G(t) = G_1(t) + G_2(t) + G_3(t) \tag{25}$$

where

$$G_1(t) = \frac{k_b^2}{\pi}\tan\left(\frac{\pi[e(t)]^2}{2k_b^2}\right) + \frac{1}{2}M\big[y(t)\big]^2 + \frac{1}{2}\tilde{D}^2 \tag{26}$$

$$G_2(t) = \frac{1}{2}\rho\int_0^N [\dot{w}(s, t)]^2 ds + \frac{1}{2}EI\int_0^N \big[w''(s, t)\big]^2 ds + \frac{1}{2}T\int_0^N \big[w'(s, t)\big]^2 ds \tag{27}$$

$$G_3(t) = \alpha\rho\int_0^N x\dot{w}(s, t)w'(s, t)ds \tag{28}$$

where $\alpha > 0$. Define an auxiliary item $y(t)$ as

$$y(t) = w'(N, t) + a_1\dot{w}(N, t) - a_2w'''(N, t) \tag{29}$$

where $a_1 > 0$, $a_2 > 0$.

Let $\mu = (\pi[e(t)]^2/2k_b^2)$. The symbols (N, t) and (s, t) are simplified to (N) and (s), respectively.

The time derivative of $G(t)$ is

$$\dot{G}(t) = \dot{G}_1(t) + \dot{G}_2(t) + \dot{G}_3(t). \tag{30}$$

The first-order derivative of (26) concerning time t is

$$\begin{aligned}\dot{G}_1(t) &= \frac{k_b^2}{\pi}\sec^2\mu \cdot \frac{\pi}{2k_b^2} \cdot 2e(t) \cdot \dot{e}(t) + My(t)\dot{y}(t) \\ &\quad + \tilde{D}\dot{\tilde{D}} \\ &= e(t)\dot{e}(t)\sec^2\mu + My(t)\dot{y}(t) + \tilde{D}\dot{\tilde{D}}.\end{aligned} \tag{31}$$

Given that the boundary position error $e(t) = w(N, t) - w_d$, where w_d is a constant, it follows that $\dot{e}(t) = \dot{w}(N, t)$. Equation (31) is denoted as

$$\dot{G}_1(t) = e(t)\dot{w}(N)\sec^2\mu + My(t)\dot{y}(t) + \tilde{D}\dot{\tilde{D}}. \tag{32}$$

Combining (14) with (27), we can obtain the derivative of $G_2(t)$ as follows:

$$\begin{aligned}\dot{G}_2(t) &= -EI\dot{w}(N)w'''(N) + T\dot{w}(N)w'(N) \\ &\quad + \int_0^N \dot{w}(s)f(s)ds - c\int_0^N [\dot{w}(s)]^2 ds.\end{aligned} \tag{33}$$

The time derivative of (28) is

$$\begin{aligned}\dot{G}_3(t) &= \alpha\rho\int_0^N s\ddot{w}(s)w'(s)ds \\ &\quad + \alpha\rho\int_0^N s\dot{w}(s)\dot{w}'(s)ds.\end{aligned} \tag{34}$$

Substituting system (16) into the above, equation (34) can be re-expressed as

$$\begin{aligned}\dot{G}_3(t) &= \alpha\rho\int_0^N s\dot{w}(s)\dot{w}'(s)ds + \alpha T\int_0^N sw''(s)w'(s)ds\\&\quad+\alpha\int_0^N sf(s)w'(s)ds - \alpha c\int_0^N s\dot{w}(s)w'(s)ds\\&\quad-\alpha EI\int_0^N xw''''(s)w'(s)ds.\end{aligned}\tag{35}$$

Based on (35) and the boundary condition (15), it is obtained that

$$\begin{aligned}\dot{G}_3(t) \le&\ -\alpha EINw'(N)w'''(N)\\&-\frac{3\alpha EI}{2}\int_0^N\left[w''(s)\right]^2ds + \frac{\alpha TN}{2}\left[w'(N)\right]^2\\&-\frac{\alpha T}{2}\int_0^N\left[w'(s)\right]^2ds + \alpha N\int_0^N f(s)w'(s)ds\\&+\frac{\alpha\rho N}{2}[\dot{w}(N)]^2 - \frac{\alpha\rho}{2}\int_0^N[\dot{w}(s)]^2ds.\end{aligned}\tag{36}$$

In combination with (32), (33), and (36), (30) is reformulated as

$$\begin{aligned}\dot{G}(t) \le&\ e(t)\dot{w}(N)\sec^2\mu + My(t)\dot{y}(t) - EI\dot{w}(N)w'''(N)\\&+\tilde{D}\dot{\hat{D}} + T\dot{w}(N)w'(N) + \int_0^N\dot{w}(s)f(s)ds\\&-c\int_0^N[\dot{w}(s)]^2ds - \alpha EINw'(N)w'''(N)\\&+\frac{\alpha TN}{2}\left[w'(N)\right]^2 - \frac{3\alpha EI}{2}\int_0^N\left[w''(s)\right]^2ds\\&-\frac{\alpha T}{2}\int_0^N\left[w'(s)\right]^2ds + \alpha N\int_0^N f(s)w'(s)ds\\&-\frac{\alpha\rho}{2}\int_0^N[\dot{w}(s)]^2ds + \frac{\alpha\rho N}{2}[\dot{w}(N)]^2.\end{aligned}\tag{37}$$

Using Lemma 3, the following relationships can be obtained

$$\int_0^N\dot{w}(s)f(s)ds \le \varepsilon_1\int_0^N[\dot{w}(s)]^2ds + \frac{1}{\varepsilon_1}\int_0^N\left[f(s)\right]^2ds\tag{38}$$

$$\begin{aligned}\alpha N\int_0^N f(s)w'(s)ds \le&\ \alpha N\varepsilon_2\int_0^N\left[w'(s)\right]^2ds\\&+\frac{\alpha N}{\varepsilon_2}\int_0^N\left[f(s)\right]^2ds\end{aligned}\tag{39}$$

where $\varepsilon_i > 0$, $i = 1, 2, 3$.

Taking (38), (39) into (37), we can get

$$\begin{aligned}\dot{G}(t) \le&\ e(t)\dot{w}(N)\sec^2\mu + My(t)\dot{y}(t) - EI\dot{w}(N)\\&\times w'''(N) + \tilde{D}\dot{\hat{D}} + T\dot{w}(N)w'(N)\\&-\alpha EINw'(N)w'''(N) - \left(c - \varepsilon_1 + \frac{\alpha\rho}{2}\right)\\&\times\int_0^N[\dot{w}(s)]^2ds - \left(\frac{\alpha T}{2} - \alpha N\varepsilon_2\right)\int_0^N\left[w'(s)\right]^2ds\\&+\left(\frac{1}{\varepsilon_1} + \frac{\alpha N}{\varepsilon_2}\right)\int_0^N\left[f(s)\right]^2ds + \frac{\alpha TN}{2}\left[w'(N)\right]^2\\&-\frac{3\alpha EI}{2}\int_0^N\left[w''(s)\right]^2ds + \frac{\alpha\rho N}{2}[\dot{w}(N)]^2.\end{aligned}\tag{40}$$

When constructing $\dot{G}(t) \le -\Theta G(t) + \delta$, there exists a coupling term $-EI\dot{w}(N)w'''(N)$ that cannot be disregarded during the PDEs computing process. In order to address this challenge, we deform the defined auxiliary term $y(t)$ to

$$\begin{aligned}\frac{EI}{2a_1a_2}\left[y(t)\right]^2 =&\ \frac{EI}{2a_1a_2}\left[w'(N)\right]^2 - \frac{EI}{a_1}w'(N)w'''(N)\\&-EI\dot{w}(N)w'''(N) + \frac{EI}{a_2}w'(N)\dot{w}(N)\\&+\frac{EIa_2}{2a_1}\left[w'''(N)\right]^2 + \frac{EIa_1}{2a_2}[\dot{w}(N)]^2.\end{aligned}\tag{41}$$

So, substituting (41) into (40), we get

$$\begin{aligned}\dot{G}(t) =&\ e(t)\dot{w}(N)\sec^2\mu + My(t)\dot{y}(t) + \tilde{D}\dot{\hat{D}}\\&+\frac{EI}{2a_1a_2}\left[y(t)\right]^2 - \frac{EI}{2a_1a_2}\left[w'(N)\right]^2\\&-\frac{EIa_1}{2a_2}[\dot{w}(N)]^2 - \frac{EIa_2}{2a_1}\left[w'''(N)\right]^2\\&-\frac{EI}{a_2}w'(N)\dot{w}(N) + T\dot{w}(N)w'(N)\\&+\left(\frac{EI}{a_1} + \alpha EIN\right)w'(N)w'''(N)\\&-\left(c - \varepsilon_1 + \frac{\alpha\rho}{2}\right)\int_0^N[\dot{w}(s)]^2ds\\&-\left(\frac{\alpha T}{2} - \alpha N\varepsilon_2\right)\int_0^N\left[w'(s)\right]^2ds\\&-\frac{3\alpha EI}{2}\int_0^N\left[w''(s)\right]^2ds + \frac{\alpha TN}{2}\left[w'(N)\right]^2\\&+\left(\frac{1}{\varepsilon_1} + \frac{\alpha N}{\varepsilon_2}\right)\int_0^N\left[f(s)\right]^2ds\\&+\frac{\alpha\rho N}{2}[\dot{w}(N)]^2.\end{aligned}\tag{42}$$

Employing Lemma 3, the subsequent relations can be derived

$$e(t)\dot{w}(N)\sec^2\mu \le \varepsilon_3\left[e(t)\sec^2\mu\right]^2 + \frac{1}{\varepsilon_3}[\dot{w}(N)]^2\tag{43}$$

$$-\frac{EI}{a_2}w'(N)\dot{w}(N) \le \frac{1}{\varepsilon_4}\frac{EI}{a_2}[\dot{w}(N)]^2 + \varepsilon_4\frac{EI}{a_2}\left[w'(N)\right]^2\tag{44}$$

$$\begin{aligned}\left(\frac{EI}{a_1} + \alpha EIN\right)w'(N)w'''(N) \le&\ \varepsilon_5\left(\frac{EI}{a_1} + \alpha EIN\right)\\&\times\left[w'(N)\right]^2 + \frac{1}{\varepsilon_5}\left(\frac{EI}{a_1} + \alpha EIN\right)\left[w'''(N)\right]^2\end{aligned}\tag{45}$$

$$T\dot{w}(N)w'(N) \le T\varepsilon_6[\dot{w}(N)]^2 + \frac{TN}{\varepsilon_6}\int_0^N\left[w''(s)\right]^2ds\tag{46}$$

where $\varepsilon_i > 0$, $i = 3, \ldots, 6$.

By invoking (43)–(46) and integrating them into (42), one obtains

$$\begin{aligned}\dot{G}(t) \le&\ \varepsilon_3\left[e(t)\sec^2\mu\right]^2 + \frac{EI}{2a_1a_2}\left[y(t)\right]^2\\&-\left(\frac{EIa_1}{2a_2} - \frac{1}{\varepsilon_3} - \frac{EI\varepsilon_4}{a_2} - \frac{\alpha\rho N}{2} - T\varepsilon_6\right)[\dot{w}(N)]^2\\&-\left(\frac{EIa_2}{2a_1} - \frac{1}{\varepsilon_5}\left(\frac{EI}{a_1} + \alpha EIN\right)\right)\left[w'''(N)\right]^2\\&-\left(\frac{EI}{2a_1a_2} - \frac{EI}{a_2\varepsilon_4} - \varepsilon_5\left(\frac{EI}{a_1} + \alpha EIN\right) - \frac{\alpha TN}{2}\right)\end{aligned}$$

$$\times\left[w'(N)\right]^2-\left(c-\varepsilon_1+\frac{\alpha\rho}{2}\right)\int_0^N[\dot{w}(s)]^2ds$$
$$+My(t)\dot{y}(t)-\left(\frac{\alpha T}{2}-\alpha N\varepsilon_2\right)\times\int_0^N\left[w'(s)\right]^2ds$$
$$-\left(\frac{3\alpha EI}{2}-\frac{TN}{\varepsilon_6}\right)\int_0^N\left[w''(s)\right]^2ds+\left(\frac{1}{\varepsilon_1}+\frac{\alpha N}{\varepsilon_2}\right)$$
$$\times\int_0^N\left[f(s)\right]^2ds+\tilde{D}\dot{\tilde{D}}. \tag{47}$$

Combining the boundary condition (16), (29) can be reformulated as

$$M\dot{y}(t)=M\dot{w}'(N)+a_1M\ddot{w}(N)-a_2M\dot{w}'''(N)$$
$$=M\dot{w}'(N)-a_2M\dot{w}'''(N)+a_1\Big(u(t)+d(t)$$
$$-d_s\dot{w}(N)+EIw'''(N)-Tw'(N)\Big). \tag{48}$$

Summarizing the above equations, we derive

$$\dot{G}(t)\le\varepsilon_3\Big[e(t)\sec^2\mu\Big]^2+\frac{EI}{2a_1a_2}\Big[y(t)\Big]^2-\Bigg(\frac{EIa_1}{2a_2}$$
$$-\frac{1}{\varepsilon_3}-\frac{EI\varepsilon_4}{a_2}-\frac{\alpha\rho N}{2}-T\varepsilon_6\Bigg)[\dot{w}(N)]^2$$
$$-\left(\frac{EIa_2}{2a_1}-\frac{1}{\varepsilon_5}\left(\frac{EI}{a_1}+\alpha EIN\right)\right)\left[w'''(N)\right]^2$$
$$-\Bigg(\frac{EI}{2a_1a_2}-\frac{EI}{a_2\varepsilon_4}-\varepsilon_5\left(\frac{EI}{a_1}+\alpha EIN\right)$$
$$-\frac{\alpha TN}{2}\Bigg)\left[w'(N)\right]^2+y(t)\big(M\dot{w}'(N)$$
$$\big(-a_2M\dot{w}'''(N)+a_1(u(t)+d(t)$$
$$-d_s\dot{w}(N)+EIw'''(N)-Tw'(N))\big)$$
$$-\left(\frac{\alpha T}{2}-\alpha N\varepsilon_2\right)\int_0^N\left[w'(s)\right]^2ds$$
$$-\left(c-\varepsilon_1+\frac{\alpha\rho}{2}\right)\int_0^N[\dot{w}(s)]^2dx$$
$$+\left(\frac{1}{\varepsilon_1}+\frac{\alpha N}{\varepsilon_2}\right)\int_0^N\left[f(s)\right]^2ds+\tilde{D}\dot{\tilde{D}}$$
$$-\left(\frac{3\alpha EI}{2}-\frac{TN}{\varepsilon_6}\right)\int_0^N\left[w''(s)\right]^2ds. \tag{49}$$

Then, the controller $u(t)$ and the adaptive law $\hat{D}$ are designed as

$$u(t)=d_s\dot{w}(N)-EIw'''(N)+Tw'(N)$$
$$+\frac{1}{a_1}\Bigg[-M\dot{w}'(N)+a_2M\dot{w}'''(N)-k_1y(t)$$
$$-a_1\tanh\left(\frac{y(t)}{\xi}\right)\hat{D}+\frac{1}{y(t)}\Bigg(-k_2\tan\mu$$
$$-\varepsilon_3\left(\beta(t)\frac{e^{\phi(t)}-e^{-\phi(t)}}{e^{\phi(t)}+e^{-\phi(t)}}\sec^2\mu\right)^2\Bigg)\Bigg] \tag{50}$$
$$\dot{\hat{D}}=a_1y(t)\tanh\left(\frac{y(t)}{\xi}\right)-\tau\hat{D} \tag{51}$$

where $\tau>0$.

Bring in (50) and (51), we can rewrite (49) as

$$\dot{G}(t)\le-\left(k_1-\frac{EI}{2a_1a_2}\right)\Big[y(t)\Big]^2-k_2\tan\mu$$
$$-a_1y(t)\tanh\left(\frac{y(t)}{\xi}\right)\hat{D}+a_1y(t)d(t)$$
$$-\Bigg(\frac{EIa_1}{2a_2}-\frac{1}{\varepsilon_3}-\frac{EI\varepsilon_4}{a_2}-\frac{\alpha\rho N}{2}$$
$$-T\varepsilon_6\Bigg)[\dot{w}(N)]^2-\Bigg(\frac{EIa_2}{2a_1}-\frac{1}{\varepsilon_5}\Bigg(\frac{EI}{a_1}$$
$$+\alpha EIN\Bigg)\Bigg)\left[w'''(N)\right]^2-\Bigg(\frac{EI}{2a_1a_2}-\frac{EI}{a_2\varepsilon_4}$$
$$-\varepsilon_5\left(\frac{EI}{a_1}+\alpha EIN\right)-\frac{\alpha TN}{2}\Bigg)\left[w'(N)\right]^2$$
$$-\left(\frac{3\alpha EI}{2}-\frac{TN}{\varepsilon_6}\right)\int_0^N\left[w''(s)\right]^2ds$$
$$+y(t)\tanh\left(\frac{y(t)}{\xi}\right)\tilde{D}-\tau\tilde{D}\hat{D}$$
$$-\left(\frac{\alpha T}{2}-\alpha N\varepsilon_2\right)\int_0^N\left[w'(s)\right]^2ds$$
$$-\left(c-\varepsilon_1+\frac{\alpha\rho}{2}\right)\int_0^N[\dot{w}(s)]^2ds$$
$$+\left(\frac{1}{\varepsilon_1}+\frac{\alpha N}{\varepsilon_2}\right)\int_0^N\left[f(s)\right]^2ds. \tag{52}$$

By combining (24) and (52), we get

$$\dot{G}(t)\le-\left(k_1-\frac{EI}{2a_1a_2}\right)\Big[y(t)\Big]^2-k_2\tan\mu$$
$$-a_1y(t)\tanh\left(\frac{y(t)}{\xi}\right)\tilde{D}+0.2785\xi a_1D$$
$$-\left(\frac{EIa_1}{2a_2}-\frac{1}{\varepsilon_3}-\frac{EI\varepsilon_4}{a_2}-\frac{\alpha\rho N}{2}-T\varepsilon_6\right)$$
$$\times[\dot{w}(N)]^2-\left(\frac{EIa_2}{2a_1}-\frac{1}{\varepsilon_6}\left(\frac{EI}{a_1}+\alpha EIN\right)\right)$$
$$\times\left[w'''(N)\right]^2-\Bigg(\frac{EI}{2a_1a_2}-\frac{EI}{a_2\varepsilon_4}-\varepsilon_5\Bigg(\frac{EI}{a_1}$$
$$+\alpha EIN\Bigg)-\frac{\alpha TN}{2}\Bigg)\left[w'(N)\right]^2-\tau\tilde{D}\hat{D}$$
$$+y(t)\tanh\left(\frac{y(t)}{\xi}\right)\tilde{D}-\left(\frac{\alpha T}{2}-\alpha N\varepsilon_2\right)$$
$$\times\int_0^N\left[w'(s)\right]^2ds-\left(c-\varepsilon_1+\frac{\alpha\rho}{2}\right)$$
$$\times\int_0^N[\dot{w}(s)]^2ds-\left(\frac{3\alpha EI}{2}-\frac{TN}{\varepsilon_6}\right)$$
$$\times\int_0^N\left[w''(s)\right]^2ds+\left(\frac{1}{\varepsilon_1}+\frac{\alpha N}{\varepsilon_2}\right)$$
$$\times\int_0^N\left[f(s)\right]^2ds. \tag{53}$$

Using Lemma 3, the parameter term $-\tau\tilde{D}\hat{D}$ in (52) is rewritten as

$$-\tau\tilde{D}\hat{D}\le-\frac{\tau}{2}\tilde{D}^2+\frac{\tau}{2}D^2. \tag{54}$$

According to the Lemma 2 and (54), we can rewrite (52) as

$$\dot{G}(t)\le\ -\left(k_1-\frac{EI}{2a_1a_2}\right)\Big[y(t)\Big]^2-k_2\tan\mu$$
$$-\left(\frac{EIa_2}{2a_1}-\frac{1}{\varepsilon_5}\left(\frac{EI}{a_1}+\alpha EIN\right)\right)\left[w'''(N)\right]^2$$

$$\begin{aligned}&-\left(\frac{EI}{2a_1a_2}-\frac{EI}{a_2\varepsilon_4}-\varepsilon_5\left(\frac{EI}{a_1}+\alpha EIN\right)\right.\\&\left.-\frac{\alpha TN}{2}\right)\left[w'(N)\right]^2-\left(\frac{3\alpha EI}{2}-\frac{TN}{\varepsilon_6}\right)\\&\times\int_0^N\left[w''(s)\right]^2ds-\left(\frac{EIa_1}{2a_2}-\frac{1}{\varepsilon_3}-\frac{EI\varepsilon_4}{a_2}\right.\\&\left.-\frac{\alpha\rho N}{2}-T\varepsilon_6\right)[\dot{w}(N)]^2+0.2785\xi a_1D\\&-\left(c-\varepsilon_1+\frac{\alpha\rho}{2}\right)\int_0^N[\dot{w}(s)]^2ds-\left(\frac{\alpha T}{2}\right.\\&\left.-\alpha N\varepsilon_2\right)\int_0^N\left[w'(s)\right]^2ds+\left(\frac{1}{\varepsilon_1}+\frac{\alpha N}{\varepsilon_2}\right)\\&\times\int_0^N\left[f(s)\right]^2ds-\frac{\tau}{2}\tilde{D}^2+\frac{\tau}{2}D^2\\\leq&-\eta_1\left[y(t)\right]^2-k_2\tan\mu-\eta_2\int_0^N[\dot{w}(s)]^2ds\\&-\eta_3\int_0^N\left[w'(s)\right]^2ds-\eta_4\int_0^N\left[w''(s)\right]^2ds\\&-\frac{\tau}{2}\tilde{D}^2+\delta\end{aligned}\tag{55}$$

where $a_1, a_2, \alpha, k_1, k_2 > 0$, $\varepsilon_i (i = 1, \ldots, 6)$ are chosen such that

$$\frac{EIa_1}{2a_2}-\frac{1}{\varepsilon_3}-\frac{EI\varepsilon_4}{a_2}-\frac{\alpha\rho N}{2}-T\varepsilon_6\geq 0\tag{56}$$

$$\frac{EIa_2}{2a_1}-\frac{1}{\varepsilon_5}\left(\frac{EI}{a_1}+\alpha EIN\right)\geq 0\tag{57}$$

$$\frac{EI}{2a_1a_2}-\frac{EI}{a_2\varepsilon_4}-\varepsilon_5\left(\frac{EI}{a_1}+\alpha EIN\right)-\frac{\alpha TN}{2}\geq 0\tag{58}$$

$$\eta_1=k_1-\frac{EI}{2a_1a_2}>0\tag{59}$$

$$\eta_2=c-\varepsilon_1+\frac{\alpha\rho}{2}>0\tag{60}$$

$$\eta_3=\frac{\alpha T}{2}-\alpha N\varepsilon_2>0\tag{61}$$

$$\eta_4=\frac{3\alpha EI}{2}-\frac{TN}{\varepsilon_6}>0\tag{62}$$

$$\begin{aligned}\delta=&\left(\frac{1}{\varepsilon_1}+\frac{\alpha N}{\varepsilon_2}\right)\int_0^N\bar{F}^2ds+0.2785\xi a_1D+\frac{\tau}{2}D^2\\&<+\infty.\end{aligned}\tag{63}$$

Utilizing Lemma 1, (55) is rewritten as

$$\begin{aligned}|G_3(t)|\leq&\frac{\alpha\rho N}{2}\int_0^N\left([\dot{w}(s,t)]^2+\left[w'(s,t)\right]^2\right)ds\\\leq&\theta G_2(t)\end{aligned}\tag{64}$$

where $\theta = [\alpha\rho N/\min(\rho, EI, T)]$ is a constant.

We can obtain the following by considering (64):

$$-\theta G_2(t)\leq G_3(t)\leq\theta G_2(t).\tag{65}$$

Select α to guarantee that $\theta \in (0, 1)$, hence satisfying the following equations:

$$\Theta_1=1-\theta=1-\frac{\alpha\rho N}{\min(\rho,EI,T)}>0\tag{66}$$

$$\Theta_2=1-\theta=1+\frac{\alpha\rho N}{\min(\rho,EI,T)}>1.\tag{67}$$

Further, according to (25), substituting (66) and (67), (65) can be written as

$$0\leq\Theta_1(G_1+G_2)\leq G(t)\leq\Theta_2(G_1+G_2).\tag{68}$$

Combining (55) with (68), we have

$$\begin{aligned}\dot{G}(t)\leq&-\Theta_3[G_1(t)+G_2(t)]+\delta\\\leq&-\Theta G(t)+\delta\end{aligned}\tag{69}$$

where $\Theta_3 = \min([2\eta_1/M], k_2, (2\eta_2/\rho), 3\alpha, [2\eta_3/T], \tau)$ and $\Theta = (\Theta_3/\Theta_2)$.

Remark 1: As stated in (9), β_∞ is the highest permissible error of $e(t)$ in a stable condition. The maximum overshoot must not surpass $\beta(0)$. Once the Lyapunov analysis theorem proves that $\phi(t)$ is bounded, the transient performance of $e(t)$ is guaranteed.

Theorem 1: Consider the flexible riser system (16) and the boundary conditions (15) and (16). Under Assumptions 1 and 2, using the designed boundary controller (50) and the adaptive law (51), the following properties are established.

1) The system boundary position $w(N, t)$ satisfies the constraints and is bounded.
2) $e(t) < \beta(t)$ holds the time, i.e., the system achieves the prescribed performance.

Proof: Multiply both sides of (69) by $e^{\Theta t}$, and integrate the equation to get

$$G(t)\leq G(0)e^{-\Theta t}+\frac{\delta}{\Theta}\left(1-e^{-\Theta t}\right).\tag{70}$$

Utilizing Lemma 1 and $\Theta_1(G_1 + G_2 + G_3) \leq G(t)$, we get

$$\frac{1}{2N}\rho[w(s)]^2\leq\frac{1}{2}\rho\int_0^N[\dot{w}(s)]^2ds\leq G_b(t)\leq\frac{1}{\Theta_1}G(t).\tag{71}$$

According to (70) and (71), we get

$$|w(s)|\leq\sqrt{\frac{2N}{\rho\Theta_1}\left(G(0)e^{-\Theta t}+\frac{\delta}{\Theta}\left(1-e^{-\Theta t}\right)\right)}.\tag{72}$$

Further, we obtain

$$\lim_{t\to\infty}|w(s)|\leq\sqrt{\frac{2N\delta}{\rho\Theta_1\Theta}}.\tag{73}$$

The boundedness of the system's kinetic and potential energies lead to the conclusion that G_1 is bounded. When $G_1 \to \infty$, $|e(t)| \to k_b$. And $|e(t)| \neq k_b$. Through the definition of G_1, we can obtain $|e(t)| < k_b$. Since $e(t) = w(N, t) - w_d$, it further follows that $|w(N, t)| \leq |w_d| + k_b$. That is, the system boundary position $w(N, t)$ satisfies the bounds of the constraint.

Since $G(t)$ is bounded, $\phi(t)$ is bounded. Further, $|e(t)| < \beta(t)$ holds. Consequently, the boundary positions converge to the specified region at the specified rate.

Furthermore, the process of selecting the appropriate parameters k_1 and k_2 is as follows. First, calculate a carefully appropriate k_1 to satisfy the condition $\eta_1 > 0$ mentioned in (59). In the simulation part, after selecting an appropriate k_1, the value of k_2 is adjusted to improve the transient response of the system. ■

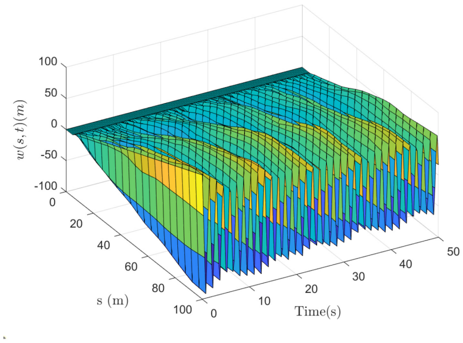

Fig. 2. Trajectories of elastic deflection $w(s, t)$ without control.

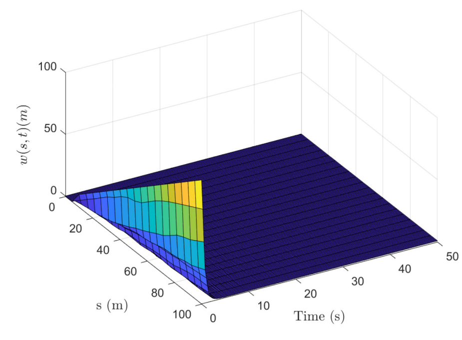

Fig. 3. Trajectories of elastic deflection $w(s, t)$ under controller (50).

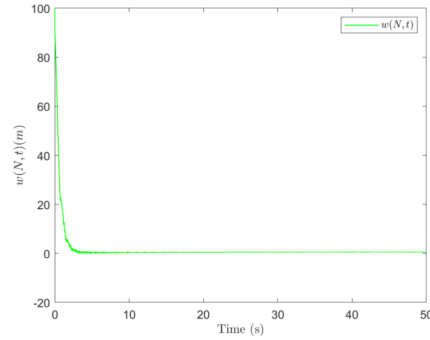

Fig. 4. Trajectory of the boundary position $w(N, t)$.

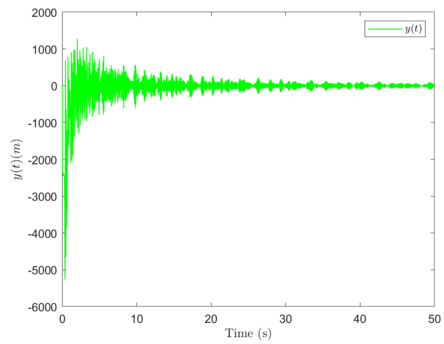

Fig. 5. Trajectory of the auxiliary item $y(t)$.

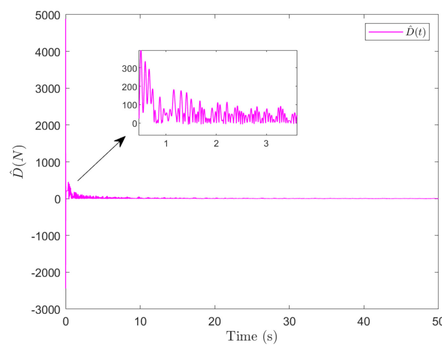

Fig. 6. Trajectory of the adaptive law $\hat{D}$.

IV. Simulation Examples

Considering the flexible riser system (14)–(16) modeled by PDEs, the backward difference method is used to verify the control performance of the system. To better demonstrate the applicability of the proposed method, two examples are presented below.

A. Flexible Riser Systems With Different Transient Properties

We not only compared the effects of various performance functions on the system in this example, but also contrasted our proposed method with the approach presented in [22].

The relevant parameters of the system are $\rho = 500$ kg/m, $h = 100$ m, $EI = 1.5 * 10^5$ N/m^2, $T = 3 * 10^7$ Ns/m, $M = 10^3$ kg, $d_s = 100$ Ns/m and $c = 3$ Ns/m^2. The parameters are selected as $a_1 = 26$, $a_2 = 1.1$, $\xi = 20$, $\varepsilon_3 = 0.02$, $\tau = 0.5$, $k_b = 100$, $k_1 = 0.011$, $k_2 = 0.07$.

Three performance functions are selected to prepare for the simulation, comparing the effects of β_0 and l in (19) on the controller, respectively, i.e.,

$$\begin{cases} \beta(t) = (90 - 2)e^{-2*10^{-3}t} + 2 \\ \beta_1(t) = (50 - 2)e^{-2*10^{-3}t} + 2 \end{cases}$$
$$\begin{cases} \beta(t) = (90 - 2)e^{-2*10^{-3}t} + 2 \\ \beta_2(t) = (90 - 2)e^{-6*10^{-3}t} + 2 \end{cases}.$$

The current distribution disturbance $f(s, t) = (\sin(10^4\pi st) + \cos(2*10^4\pi st) + \sin(3*10^4\pi st) + 10^4)/(100h)$. The external boundary disturbance $d(t) = (2\sin(5t) + 3\sin(2t)) * 10^3$.

Figs. 2 and 3 show the positions $w(s, t)$ of the system with and without control. Through image comparison, it can be observed that position $w(s, t)$ rapidly converges to the intercell zero with control, and the convergence rate is significantly better than that without control, demonstrating the effectiveness of the control. Fig. 4 shows the trajectory of boundary position $w(N, t)$ when the parameters are unknown. It can be seen that $w(N, t)$ quickly stabilizes within 5 s, achieving good control performance. Fig. 5 shows the designed auxiliary item $y(t)$. Fig. 6 shows the adaptive law $\hat{D}$. It can be observed that these trajectories tend to stabilize within a short period of time.

Fig. 7 shows the error after transformation. We make two comparisons of the error after the transformation. In Group 1, the red line represents the change trajectory under $\beta(t) = (90 - 2)e^{-2*10^{-3}t} + 2$, and the green line represents the change trajectory under $\beta_1(t) = (300 - 2)e^{-2*10^{-3}t} + 2$. It is clear that the red trajectory is better than the green trajectory. In Group 2, the red line represents the change trajectory under $\beta(t) = (90 - 2)e^{-2*10^{-3}t} + 2$, and the green line represents

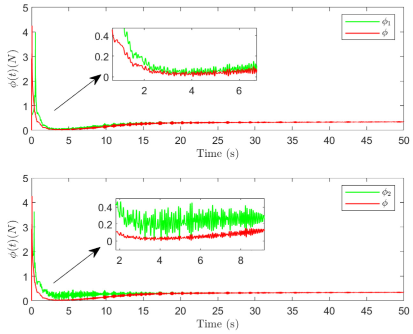

Fig. 7. Trajectory of the error after transformation $\phi(t)$.

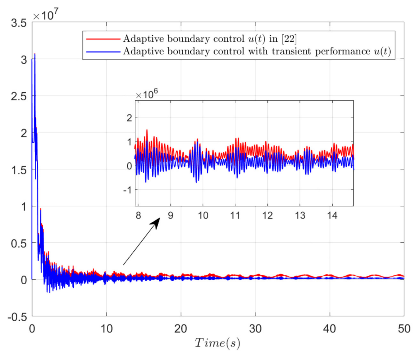

Fig. 8. Trajectory of boundary controller $u(t)$ under [22] and proposed control method.

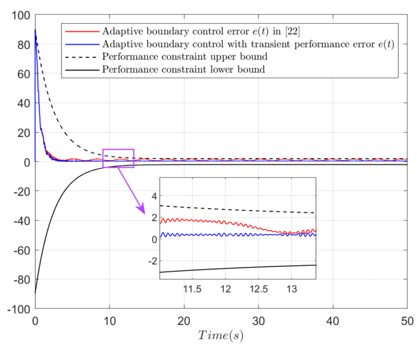

Fig. 9. Trajectory of boundary position error $e(t)$ under [22] and proposed control method.

the change trajectory under $\beta_2(t) = (90-2)e^{-6*10^{-3}t} + 2$. Again, it is clear that the red trajectory is better than the green trajectory. By comparing the two groups, it can be concluded that the designed error after transformation is optimal when β_0 is smaller and l is smaller in $\beta(t) = (\beta_0 - \beta_\infty)e^{-lt} + \beta_\infty$.

To demonstrate the enhancement in control efficacy facilitated by transient performance control, we compared it with the method proposed in [22]. Figs. 8 and 9 compare the controller and error in [22] with the proposed control method, respectively. The red line in the figures shows the adaptive boundary control in [22], while the blue line represents the adaptive boundary control with transient performance under the proposed control method. It can be observed that the boundary controllers are fundamentally consistent in Fig. 8. Compared to the case where transient performance is not considered, the error under the proposed control methodology

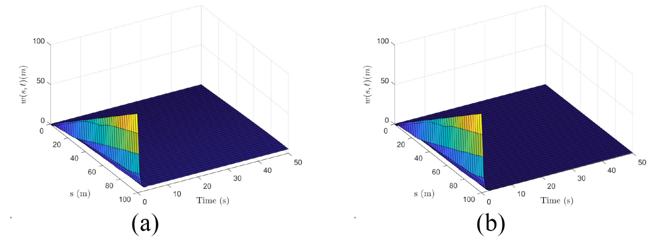

Fig. 10. Trajectories of elastic deflection $w(s,t)$ for different external disturbances under controller (50). (a) Under d_1. (b) Under d_2.

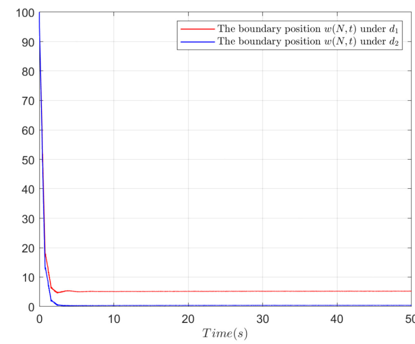

Fig. 11. Trajectories of the boundary position $w(N,t)$ for different external disturbances.

reaches steady-state more rapidly and exhibits a lower steady-state value in Fig. 9.

B. Flexible Riser Systems With Different External Disturbances

This section considers performance function and different external disturbances.

The performance function is selected as $\beta(t) = (90-10)e^{-2*10^{-3}t} + 10$. The current distribution disturbance $f(s,t)$ is shown in [36]. The external boundary disturbances

$$\begin{cases} d_1(t) = (0.5\sin(0.7t) + 0.8\cos(0.7t) + 0.2\sin(0.3t)) * 10^2 \\ d_2(t) = (2\sin(5t) + 3\cos(2t)) * 10^3. \end{cases}$$

The parameters are selected as $a_1 = 26$, $a_2 = 1.1$, $\xi = 2$, $\varepsilon_3 = 0.02$, $\tau = 0.5$, $k_b = 100$, $k_1 = 0.011$, $k_2 = 0.07$.

Fig. 10 shows the variation of the flexible riser position $w(s,t)$ under the controller (50) proposed in this article for different external disturbances and transient performance. The comparison of the images indicates that the position $w(s,t)$ can converge and stable swiftly after adopting the control strategy proposed in this article. Fig. 11 shows the trajectory of the boundary position $w(N,t)$ under different external disturbances. It can be observed that, although different external disturbances can impact the flexible riser system in this design scheme, the proposed controller effectively ensures that the system converges to the specified area at the desired rate.

Fig. 12 shows the designed auxiliary item $y(t)$. Fig. 13 shows the adaptive law $\hat{D}$. Fig. 14 shows the boundary controller $u(t)$ in (50). Fig. 15 displays the boundary position error $e(t)$ and their constraint boundaries during transient performance. These trajectories demonstrate a rapid

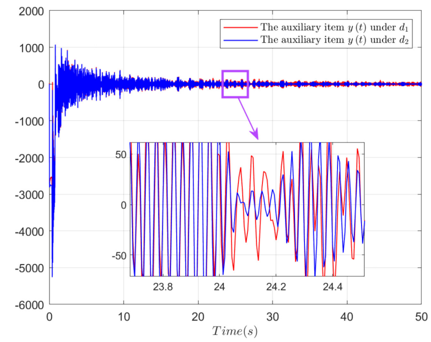

Fig. 12. Trajectories of the auxiliary item $y(t)$ for different external disturbances.

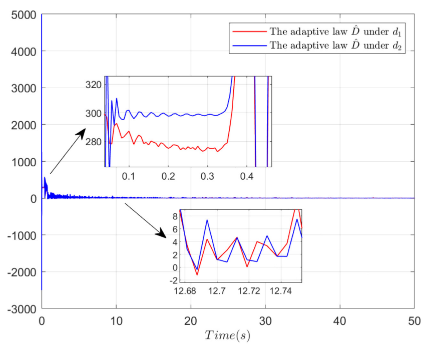

Fig. 13. Trajectories of the adaptive law $\hat{D}$ for different external disturbances.

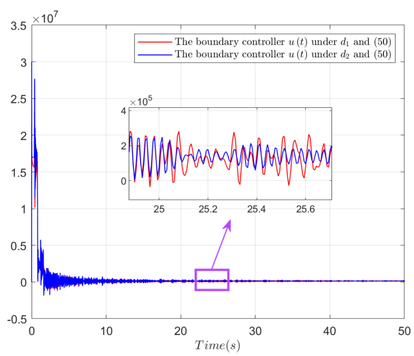

Fig. 14. Trajectories of the boundary controller $u(t)$ in (50) for different external disturbances.

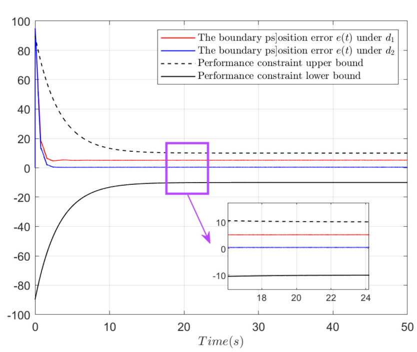

Fig. 15. Trajectories of the boundary position error $e(t)$ and constraint bounds for different external disturbances.

stabilization tendency. It can be concluded that the proposed control method remains effective under different external disturbances and performance function.

V. Conclusion

The boundary state constraint problem of an ocean riser system based on PDEs modeling has been addressed in this article to ensure transient performance and disturbance rejection. The adaptive control scheme that suppresses elastic deflection vibration has been proposed to ensure fast tracking of boundary position errors and achieve desirable transient performance. A novel boundary controller and adaptive law based on the tangent BLF have been designed to ensure signal bounding and restrict the boundary position error within its constraint range. Finally, the above scheme has been further validated by MATLAB simulations. It is noted that only constant constraints have been considered in this article. Future research will explore time-varying constraints and practical experimental results. We are planning to create a ship-based platform in the future to validate the effectiveness and applicability of the proposed method.

References

[1] Y. Zhang, F. Kong, Q. Zhu, and T. Huang, "Quantized control based on stabilization of discontinuous memristor-based fuzzy inertial neural networks with proportional delays," *IEEE Trans. Syst., Man, Cybern., Syst.*, vol. 54, no. 9, pp. 5756–5767, Sep. 2024.

[2] D. Wang, D. Liu, Q. Zhang, and D. Zhao, "Data-based adaptive critic designs for nonlinear robust optimal control with uncertain dynamics," *IEEE Trans. Syst., Man, Cybern., Syst.*, vol. 46, no. 11, pp. 1544–1555, Nov. 2016.

[3] C.-W. Kuo, C.-C. Tsai, and C.-T. Leei, "Intelligent leader-following consensus formation control using recurrent neural networks for small-size unmanned helicopters," *IEEE Trans. Syst., Man, Cybern., Syst.*, vol. 51, no. 2, pp. 1288–1301, Feb. 2021.

[4] B. Xu, X. Wang, W. Chen, and P. Shi, "Robust intelligent control of SISO nonlinear systems using switching mechanism," *IEEE Trans. Syst., Man, Cybern., Syst.*, vol. 51, no. 8, pp. 3975–3987, Aug. 2021.

[5] D. Cruz-Ortiz, I. Chairez, and A. Poznyak, "Sliding-mode control of full-state constraint nonlinear systems: A barrier Lyapunov function approach," *IEEE Trans. Syst., Man, Cybern., Syst.*, vol. 52, no. 10, pp. 6593–6606, Oct. 2022.

[6] C. Li, C. Ma, Y.-H. Chen, and R. Yu, "Stratified game-theoretic optimization of robust control design for fuzzy dynamical systems: A hybrid Nash–Stackelberg strategy," *IEEE Trans. Syst., Man, Cybern., Syst.*, vol. 54, no. 4, pp. 2287–2296, Apr. 2024.

[7] H. W. D. Hettiarachchi, K. T. M. U. Hemapala, and A. G. B. P. Jayasekara, "Review of applications of fuzzy logic in multi-agent-based control system of AC-DC hybrid microgrid," *IEEE Access*, vol. 7, pp. 1284–1299, 2019.

[8] R. Sharma, S. Bhasin, P. Gaur, and D. Joshi, "A switching-based collaborative fractional order fuzzy logic controllers for robotic manipulators," *Appl. Math. Model.*, vol. 73, pp. 228–246, Sep. 2019.

[9] S. C. Tong, Y. M. Li, G. Feng, and T. S. Li, "Observer-based adaptive fuzzy backstepping dynamic surface control for a class of MIMO nonlinear systems," *IEEE Trans. Syst., Man, Cybern. B, Cybern.*, vol. 41, no. 4, pp. 1124–1135, Aug. 2011.

[10] F. Wang, X. Zhang, B. Chen, C. Lin, X. Li, and J. Zhang, "Adaptive finite-time tracking control of switched nonlinear systems," *Inf. Sci.*, vol. 421, pp. 126–135, Dec. 2017.

[11] H.-C. Huang and C.-C. Tsai, "FPGA implementation of an embedded robust adaptive controller for autonomous omnidirectional mobile platform," *IEEE Trans. Ind. Electron.*, vol. 56, no. 5, pp. 1604–1616, May 2009.

[12] S. Tong, X. Min, and Y. Li, "Observer-based adaptive fuzzy tracking control for strict-feedback nonlinear systems with unknown control gain functions," *IEEE Trans. Cybern.*, vol. 50, no. 9, pp. 3903–3913, Sep. 2020.

[13] H. Ma, Z. Wang, D. Wang, D. Liu, P. Yan, and Q. Wei, " Neural-network-based distributed adaptive robust control for a class of nonlinear multiagent systems with time delays and external noises," *IEEE Trans. Syst., Man, Cybern., Syst.*, vol. 46, no. 6, pp. 750–758, Jun. 2016.

[14] C. Wang, Y. Wu, and J. Yu, “Barrier Lyapunov functions-based adaptive control for nonlinear pure-feedback systems with time-varying full state constraints,” *Int. J. Control, Autom. Syst.*, vol. 15, no. 6, pp. 2714–2722, Oct. 2017.

[15] Y. J. Liu and S. Tong, “Barrier Lyapunov functions-based adaptive control for a class of nonlinear pure-feedback systems with full state constraints,” *Automatica*, vol. 64, pp. 70–75, Feb. 2016.

[16] J. Zhang, S. Wang, P. Zhou, L. Zhao, and S. Li, “Novel prescribed performance-tangent barrier Lyapunov function for neural adaptive control of the chaotic PMSM system by backstepping,” *Int. J. Electr. Power Energy Syst.*, vol. 121, Oct. 2020, Art. no. 105991.

[17] Z. Li, S. Li, Y.-J. Liu, and L. Liu, “Event-triggered neural control for time-varying delay switched systems with constraints relate to historical states under average dwell time,” *IEEE Trans. Syst., Man, Cybern., Syst.*, vol. 54, no. 3, pp. 1427–1437, Mar. 2024.

[18] W. Sun, S. F. Su, G. Dong, and W. Bai, “Reduced adaptive fuzzy tracking control for high-order stochastic nonstrict feedback nonlinear system with full-state constraints,” *IEEE Trans. Syst., Man, Cybern., Syst.*, vol. 51, no. 3, pp. 1496–1506, Mar. 2021.

[19] Y.-H. Liu, Y. Liu, Y.-F. Liu, and C.-Y. Su, “Adaptive fuzzy control with global stability guarantees for unknown strict-feedback systems using novel integral barrier Lyapunov functions,” *IEEE Trans. Syst., Man, Cybern., Syst.*, vol. 52, no. 7, pp. 4336–4348, Jul. 2022.

[20] D. Li, S.-M. Lu, and L. Liu, “Adaptive NN cross backstepping control for nonlinear systems with partial time-varying state constraints and its applications to hyper-chaotic systems,” *IEEE Trans. Syst., Man, Cybern., Syst.*, vol. 51, no. 5, pp. 2821–2832, May 2021.

[21] Z. L. Tang, K. P. Tee, and W. He, “Tangent barrier Lyapunov functions for the control of output-constrained nonlinear systems,” *IFAC Proc. Vol.*, vol. 46, no. 20, pp. 449–455, 2013.

[22] F. Xu, L. Tang, and Y. J. Liu, “Tangent barrier Lyapunov function-based constrained control of flexible manipulator system with actuator failure,” *Int. J. Robust Nonlinear Control*, vol. 31, no. 7, pp. 8523–8536, Aug. 2021.

[23] T. Jiang, J. Liu, and W. He, “Adaptive boundary control for a flexible manipulator with state constraints using a barrier Lyapunov function,” *J. Dyn. Syst. Meas. Control*, vol. 140, no. 8, Mar. 2018, Art. no. 81018.

[24] Z. Ma and P. Huang, “Adaptive neural-network controller for an uncertain rigid manipulator with input saturation and full-order state constraint,” *IEEE Trans. Cybern.*, vol. 52, no. 5, pp. 2907–2915, May 2022.

[25] B. Niu and J. Zhao, “Tracking control for output-constrained nonlinear switched systems with a barrier Lyapunov function,” *Int. J. Syst. Sci.*, vol. 44, no. 5, pp. 978–985, Jan. 2013.

[26] W. Sun, S.-F. Su, Y. Wu, J. Xia, and V.-T. Nguyen, “Adaptive fuzzy control with high-order barrier Lyapunov functions for high-order uncertain nonlinear systems with full-state constraints,” *IEEE Trans. Cybern.*, vol. 50, no. 8, pp. 3424–3432, Aug. 2020.

[27] W. He, X. He, and S. S. Ge, “Vibration control of flexible marine riser systems with input saturation,” *IEEE/ASME Trans. Mechatronics*, vol. 21, no. 1, pp. 254–265, Feb. 2016.

[28] S. Zhang, P. Yang, L. Kong, G. Li, and W. He, “A single parameter-based adaptive approach to robotic manipulators with finite time convergence and actuator fault,” *IEEE Access*, vol. 8, pp. 15123–15131, 2020.

[29] J. Huang, W. Wang, and J. Zhou, “Adaptive control design for underactuated cranes with guaranteed transient performance: Theoretical design and experimental verification,” *IEEE Trans. Ind. Electron.*, vol. 69, no. 3, pp. 2822–2832, Mar. 2022.

[30] Z. Liu and J. Liu, “Adaptive iterative learning boundary control of a flexible manipulator with guaranteed transient performance,” *Asian J. Control*, vol. 20, no. 3, pp. 1027–1038, 2018.

[31] M. Chen, Q. Wu, C. Jiang, and B. Jiang, “Guaranteed transient performance based control with input saturation for near space vehicles,” *Sci. China Inf. Sci.*, vol. 57, no. 5, pp. 1–12, Jan. 2014.

[32] X. Bu, X. Wu, J. Huang, and D. Wei, “A guaranteed transient performance-based adaptive neural control scheme with low-complexity computation for flexible air-breathing hypersonic vehicles,” *Nonlinear Dyn.*, vol. 84, no. 4, pp. 2175–2194, Feb. 2016.

[33] W. He and S. S. Ge, “Vibration control of a flexible beam with output constraint,” *IEEE Trans. Ind. Electron.*, vol. 62, no. 8, pp. 5023–5030, Aug. 2015.

[34] L. Liu, Y. J. Liu, S. C. Tong, and Z. Gao, “Relative threshold-based event-triggered control for nonlinear constrained systems with application to aircraft wing rock motion,” *IEEE Trans. Ind. Informat.*, vol. 18, no. 2, pp. 911–921, Feb. 2022.

[35] Z. Zhao, X. He, Z. Ren, and G. Wen, “Output feedback stabilization for an axially moving system,” *IEEE Trans. Syst., Man, Cybern., Syst.*, vol. 49, no. 12, pp. 2374–2383, Dec. 2019.

[36] W. He, S. S. Ge, B. V. E. How, Y. S. Choo, and K.-S. Hong, “Robust adaptive boundary control of a flexible marine riser with vessel dynamics,” *Automatica*, vol. 47, no. 4, pp. 722–732, Apr. 2011.